Hindawi Publishing Corporation
International Journal of Corrosion
Volume 2012, Article ID 301392, 8 pages
doi:10.1155/2012/301392

Research Article

Study of Zn-Ni Alloy Coatings Modified by Nano-SiO_2 Particles Incorporation

Olfa Hammami,[1,2] Leila Dhouibi,[1] Patrice Berçot,[2] El Mustafa Rezrazi,[2] and Ezzeddine Triki[1]

[1] *Unit of Research "COPROMET" ENIT, University of Tunis-El Manar, BP 371002 Belvedere, Tunisia*
[2] *Institut UTINAM, CNRS UMR 6213, Équipe Sonochimie et Réactivité des Surfaces, Université de Franche-Comté, 16 Route de Gray, 25030 Besançon Cedex, France*

Correspondence should be addressed to Olfa Hammami, holfa@rocketmail.com

Received 5 August 2011; Accepted 20 November 2011

Academic Editor: F. J. M. Pérez

The aim of this research work was to codeposit nano-SiO_2 particles into Zn-Ni alloy coatings in order to improve some surface properties. It had been investigated the effect of loading the plating bath with nanoparticles on composition, morphology, phase structure of deposits, and their subsequent influence on the corrosion process in corrosive solution of 3% NaCl and the thermal stability of deposits at 200°C. It was found that Zn-Ni alloy composites contain a higher percentage of Ni with incorporation in the deposit of 1.54% of silica. X-ray diffraction measurements revealed that the alloys consisted of two phases, pure zinc and γ phase. Electrochemical characterization of the composites had been carried out through potentiodynamic polarization and electrochemical impedance spectroscopy. The composites exhibited higher values of microhardness and better corrosion resistance in corrosive media.

1. Introduction

The need for coatings with improved resistance to highly aggressive environments is high as a result of a growing demand for extended safe service life of industrial objects. Composite electrodeposition is a valuable new surface intensification technology to obtain composite coatings allowing to codeposit inorganic and organic particles into the coatings in order to improve the surface properties. Several studies showed that electrochemically embedded particles impart special properties to composite coatings produced, which can meet the industrial request such as wear resistance, self-lubrication, and corrosion resistance [1–3]. Currently and for the foreseeable future, the most important types of nanoparticles are simple oxides, such as Al_2O_3, TiO_2, and SiO_2 used in established applications [4–6]. The electrodeposition of Zn-Ni-SiO_2 has generated amount of interest in the past years due to the attractive properties of Zn-Ni-SiO_2 coating, the introduction of this alloy into industrial practice has been extremely successful. In addition, it has been observed that varying the electroplating bath chemistry, conditions, and deposition parameters may give rise to a wide variation in properties of the resulting deposits.

Zn-Ni-SiO_2 coating has recently been used to replace cadmium plating which is widely used in the aerospace industries (i.e., landing gear, hydraulic actuators, high-performance fasteners, break, and fuel lines) because of its excellent corrosion resistance. The relation between our work and existing works on Zn-Ni-SiO_2 composite coating is to replace the coating with Zn-Ni-SiO_2 alloy as this coating shows great promise from the corrosion resistance point of view, representing a real challenge. Zn-Ni-SiO_2 coating system may also find a wide range of advanced applications in marine industry, so we found it interesting to study this type of composite coating in 3% NaCl.

The particles of SiO_2 are hydrophilic and hence incorporate hardly into the surface of cathode. The main purpose of this research work was to codeposit nano-SiO_2 particles into the Zn-Ni alloy coatings under direct current in order to improve the surface properties and the corrosion resistance in aggressive media.

Table 1: Solution composition and conditions for alloy electroplating [7].

Electrolyte ingredients	Concentration ($g \cdot L^{-1}$)	Plating parameters	$R = [Zn^{2+}]/[Ni^{2+}]$
$ZnSO_4 \cdot 7H_2O$	57.5		
$NiSO_4 \cdot 6H_2O$	52.5	pH = 2, 5	
H_3BO_3	9.3	Temperature (°C):	1.1
Na_2SO_4	56.8	30 ± 0.5	
H_2SO_4	0.53		

Then, the composite coatings had been characterized from compositional (EDX), morphological (SEM), structural (XRD), and depth profile (GDOES) points of view. In the meantime, electrochemical properties of the composite coatings had been studied by potentiodynamic polarization and electrochemical impedance spectroscopy.

Table 2: Electrophoretic mobility and Zeta potential measurements by "Rank Brother II".

pH of bath solution	Effective charge of SiO_2 particles	Electrophoretic mobility ($cm^2 \cdot V^{-1} \cdot s^{-1}$)	Zeta potential (mV)
6.7	—	1.45×10^{-8}	18.6

2. Experimental

2.1. Electroplating Process. The chemical compositions of the basic electrolyte of Zn-Ni alloys deposition is given in Table 1 [7]. All experiments were carried out in duplicates, and the ability to reproduce of these measurements was found satisfactory.

Galvanostatic measurements were performed on steel rod cathode which was placed in a PTFE mount for obtaining cross-sectional area of 0.2 cm^2 in contact with solution. The deposition was done on steel (STUB 100CR6) substrates. The chemical composition of STUB 100CR6 steel was 98.6% Fe, 0.95% C, 0.2%, Mn 0.15% Si, and 0.015% S (wt%). Initially, the steel samples were mechanically polished with successively finer grades of emery paper. They were then washed in deionized water. This procedure was repeated until a clear and smooth surface was obtained. To obtain fixed hydrodynamic conditions, the Zn-Ni coatings were deposited on a rotating disc electrode (RDE) with a constant rotation velocity of 1000 rpm. The deposition experiments were performed at a current density of 25 mA/cm^2, and the plating time was 15 min. The SiO_2 powder (AEROSIL 200) with a mean diameter of 12 nm was used as received without any pretreatment.

Before electrodeposition, the nanoparticles were dispersed in the bath by ultrasonic wave for 30 min. Particles with concentration of 5 g/L were maintained in an electrolytic bath in suspension by continuous magnetic stirring of 200 rpm for at least 24 hours before deposition.

2.2. Elesctrochemical Measurements. For electrochemical measurements (anodic polarization curves and impedance spectra), the coated samples were exposed to 3% NaCl solution (pH $= 7 \pm 0.1$, $T = 25°C$). These studies were performed respectively with potentiostat PGP 201 and interface Solartron SI 1287/SI 1250 in a thermostatic three-electrode cell. The working electrode was a coated sample, the counter electrode was platinum with an area of 1 cm^2 and the reference electrode was saturated calomel SCE ($Hg/Hg_2Cl_2/KCl$ saturated). The deposition and potentiodynamic stripping processes were performed in a nonagitated electrolyte at room temperature.

2.3. Characterization Studies. An X-ray diffraction investigation of Zn-Ni electrodeposits was carried out using an X-ray diffractometer D8 (Advance Bruker) equipped with a copper anode generating Ni-filtered CuKα radiation (l = 1.5405 Å, 45 KV, 40 mA). The quantity of Zn and Ni in the coatings and their thicknesses was determined by means of Fischerscope X-Ray XDAL fluorescence. Surface morphology of the deposits was followed with electron microscope at 15 KV. Measurements of the Vickers microhardness (HV) of deposits were performed in the surface by using as HMV-M3 SHIMADZU Microhardness tester under 25 g to 100 g load for 10 s, and the corresponding final values were determined as the average of 5 measurements.

Glow discharge optical emission spectroscopy (GDOES); the distribution of species in the deposit, was determined by depth profiling using a Jobin Yvon GD-Profiler instrument equipped with a 4 mm diameter anode and operating after optimization at a pressure of 650 Pa and a power of 30 W in an argon atmosphere. This low power was retained to decrease the speed of abrasion of the deposits with low thickness and to obtain maximum information at the surface. Quantified compositional results were evaluated automatically utilizing the standard Jobin Yvon quantum Intelligent Quantification software. The instrument was calibrated with standard known composition. Depths were calculated using relative sputter rates, obtained from the sputter yields of each major element with corrections for composition and discharge conditions.

3. Results and Discussion

3.1. Behavior of SiO_2 Nanoparticles in the Plating Solution. In Table 2, we regrouped zeta potential and electrophoretic mobility measurements of particles suspended in the electroplated solution diluted 100 times. By observing the movement of particles under the influence of an electric field in

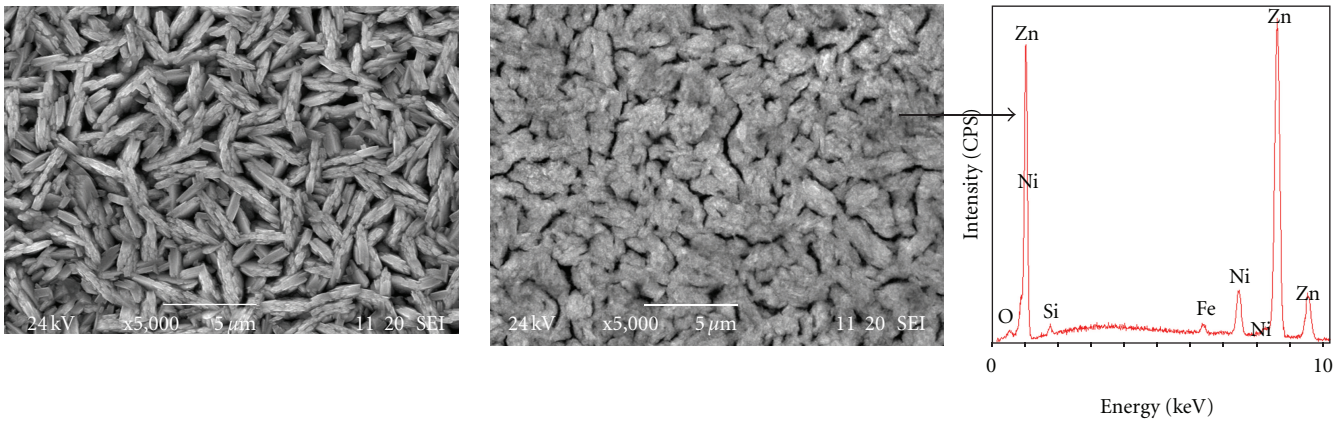

(a) (b)

Figure 1: SEM micrographs and EDS of the surfaces of Zn-Ni-coated steel at 25 mA/cm^2 for 15 min in plating bath: (a) Zn-Ni alloy coating, (b) Zn-Ni alloy composite (with 5 g/L SiO_2).

the airframe microelectrophoresis "Rank Brothers II," we can determine the effective charge of particles and calculate the electrophoretic mobility of the particle and its corresponding zeta potential.

We noted negatively charged particles of SiO_2. This type of oxide is hydrophilic, so it always interacts with the electrolyte, and therefore chemical and physical adsorption of electrolyte ions onto the particle occurs. This adsorption and the initial particle surface composition determine the particle surface charge, which induces a double layer of electrolyte ions around the particle. In electrolytes, double layers play a major role in the interactions between particles and also between particles and the electrode [8]. SiO_2 has a negative surface charge at pH 6.7, and therefore zinc or nickel ions should surround the particles to give them an overall positive surface charge. According to some authors, this may lead to codeposition at the negatively charged cathode [9].

The absolute value of the zeta potential is a very important factor for the degree of particles incorporation. In fact, zeta potential determined the static electricity force among nano-SiO_2 particles and influenced greatly the character either agglomeration or dispersion among the nanoparticles [10]. When the nanoparticles of SiO_2 became close to the cathode, the repulsion force among the double-charge layers of nanoparticles and increased the possibility of conglobation among nanoparticles decreased. In addition, the positive/negative of the zeta potential value on the nanoparticle surfaces had the crucial influence to the interaction among nanoparticles and cathode surface during electrodeposition. So the stability of the composite electrodeposition solution could be characterized by the zeta potential on the nanoparticle surfaces. It can be seen from Table 2 that, in pH 6.7, the value of zeta potential was lower than 25 mV, showing that, in the composite electrodeposition solution, the conglobation trend among nanoparticles increased and the dispersibility of the composite electrodeposition solution was weakened [10].

3.2. Compositional Analysis, Morphology, and Depth Profile of Deposits. Table 3 showed a comparison between Zn-Ni deposits composition electroplated at 25 mA/cm^2 for 15 min.

Table 3: Composition analysis by X-ray fluorescence of Zn-Ni deposits electroplated at 25 mA/cm^2 for 15 min onto steel substrate.

Coating systems	Ni (±0.2 wt.%)	Zn (±0.2 wt.%)	R' = Zn/Ni
Zn-Ni alloy coating	6.3	93.7	14.9
Zn-Ni/nano-SiO_2 alloy composite	12.3	87.7	7.1

The X-ray fluorescence analysis of the composite coatings revealed about a double percentage of Ni in the alloy composite in comparison with Zn-Ni alloy coating. The Ni content of Zn-Ni alloy deposits plays a major role in controlling the phases present and the grain size [11]. In the electrodeposition of Zn-Ni/SiO_2 composites, a phenomenon of induced codeposition was observed, since SiO_2 increased the percentage of Ni in the alloys, Ni cations simultaneously accelerated the codeposition of SiO_2 [12].

The ratio of the less noble metal Zn to the more noble metal Ni in the deposit (R') is larger than in the bath (R). This phenomenon is known as "anomalous codeposition," fully described by Brenner [13].

The surface morphology of Zn-Ni alloy coating showed branched acicular crystallite structure (Figure 1(a)), as proved in our anterior results [7]. The surface of the composite coating (Figure 1(b)) seems to keep the same appearance with piled and smooth grains. EDS analysis of the composite coating surface revealed a silica content of 1.54%.

Figure 2 showed the GDOES depth profile of the wt.% amount of the selected elements: zinc, nickel, silicon and iron for the Zn-Ni composite coating. The distributions of the different species are revealed clearly with sharply defined interface between the deposit and the substrate. The thickness of the composite measured by GDOES correlate very well with the one obtained by X-ray fluorescence (approximately 7 μm). Zinc and nickel species are incorporated relatively uniformly along the cross-section as depicted in Figure 2. Just in the outer region of the film, we confirm the presence of silicon which decreased until a depth of approximately 0.5 μm.

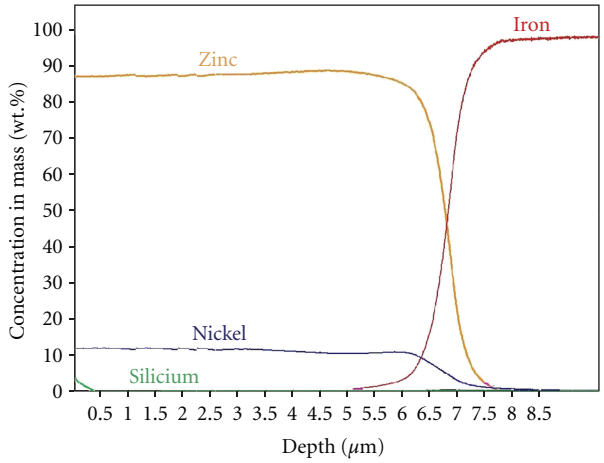

Figure 2: GDOES depth quantified profile of the Zn-Ni alloy composite (with 5 g/L SiO_2) electrodeposited with (25 mA/cm^2, 15 min) onto steel substrate.

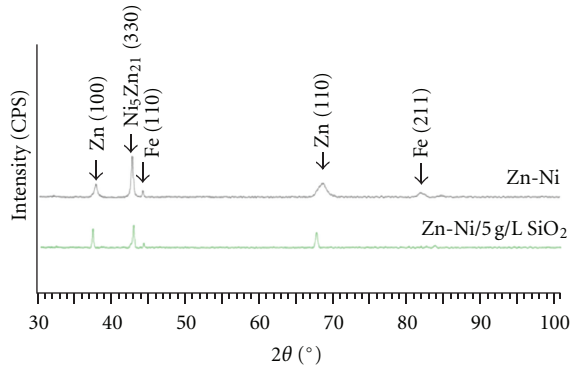

Figure 3: X-ray diffractograms for Zn-Ni alloy coating and Zn-Ni alloy composite (with 5 g/L SiO_2) electroplated at 25 mA/cm^2 for 15 min.

3.3. Phase Structure and Microhardness. Figure 3 showed the XRD patterns for the plated Zn-Ni alloy coatings. It is clear that no significant change of phases content in spectra resulted from loading the plating bath with nano-SiO_2 particles. Only the diffraction lines of zinc and γ phase of Zn-Ni alloys were observed. However, the peak of Fe (211) in the Zn-Ni/5 g/L SiO_2 alloy composite diffractogram disappeared giving rise probably to a deposit covering the surface of steel better than Zn-Ni alloy coating. We noted that Zn-Ni alloy coating and composite coating had approximately the same thicknesses.

Crystallite sizes of the coatings were calculated from the X-ray peak broadening of the (330) diffraction peak using Scherrer's formula [14]:

$$D = K\lambda/(\beta cos\theta), \quad (1)$$

where K is the Scherrer factor ≈ 1, D is the crystallite size, λ is the incident radiation wavelength, β is the integral breadth of the structurally broadened profile, and θ is the angular position.

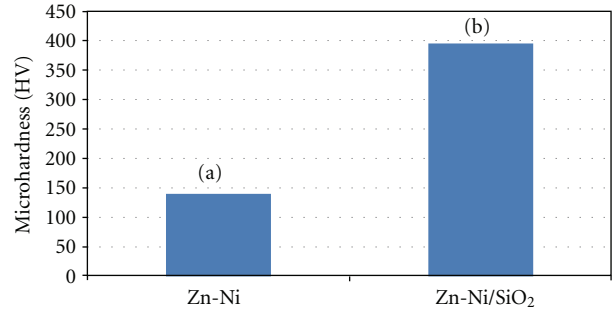

Figure 4: Evolution of microhardness of Zn-Ni alloy coatings (a) and Zn-Ni alloy composites (b) electroplated onto steel substrate at 25 mA/cm^2 for 15 min.

Zn-Ni alloy deposit exhibited a crystallite size of 50 nm, whereas the crystallite size of Zn-Ni composite coating decreased to 26 nm. We could explain this evolution by the fact that the nanoparticles of silica might perturb the crystal growth by increasing the number of nucleation sites and consequently a reduction in the grain size occurs as reported by Pavlatou et al. [1]; namely, the growth of the electrodeposited layer is a competition between the nucleation and crystal growth. Nanoparticles provide more nucleation sites and hence retard the crystal growth; subsequently the corresponding Zn-Ni matrix in the composite coating has a smaller crystal size.

Vickers microhardness (HV) values of Zn-Ni alloy deposits are shown in Figure 4.

The evolution of coatings hardness showed an increase from about 140 HV for pure Zn-Ni alloy to about 396 HV for samples prepared with SiO_2 particles. We can conclude that the microhardness was affected by the incorporation of this type of nanoparticles into deposits. In turn, crystallite size is an important variable affecting the hardness value [15]. In fact, smaller crystallite size implies a greater number of grain boundaries that impede dislocation motion and then creates harder materials.

3.4. Thermal Stability. The thermal stability of Zn-Ni alloy electrodeposits is important to their general evaluation for future applications, particularly in applications where the coatings are expected to perform at elevated temperature such as on some automotive parts. In this study, in order to evaluate the stability of the deposits, we followed the microhardness evolution of deposits treated at 200°C continuously for 30 min, 2 hours, and 24 hours (Figure 5).

After annealing at 200°C, deposits revealed reduced hardness values after 30 min of thermal treatment, especially the hardness of composites alloy. The reduced hardness could be attributed to surface oxidation phenomena or a rapid grain growth and a decrease of internal stresses as reported by Apachitei et al. [16]. Further heating for 24 hours at 200°C led to stable Vickers microhardness of composite deposits. These values were maintained higher than those of Zn-Ni alloy coatings.

Table 4: E_{corr} and peaks positions of stripping response in 3% NaCl solution for Zn-Ni alloy deposits elaborated under DC (25 mA/cm^2, 15 min).

Samples	Peak 1			Peak 2		Peak 3	
	E_{corr} ± 5 mV/SCE	E_p ± 4 mV/SCE	i_p ± 2 mA/cm^2	E_p ± 4 mV/SCE	i_p ± 2 mA/cm^2	E_p ± 4 mV/SCE	i_p ± 2 mA/cm^2
Zn-Ni alloy coating	−1020	−800	15	−615	8	−445	5
Zn-Ni alloy composite	−941	−815	5	−544	13	−404	10.5

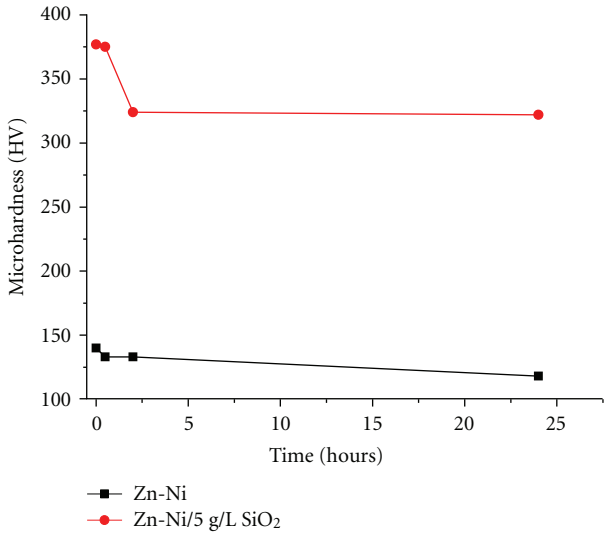

Figure 5: Variation of microhardness of Zn-Ni alloy deposit and coating composite electroplated onto steel substrate at 25 mA/cm^2 for 15 min and heat treated at 200°C for 30 min, 2 h, and 24 h.

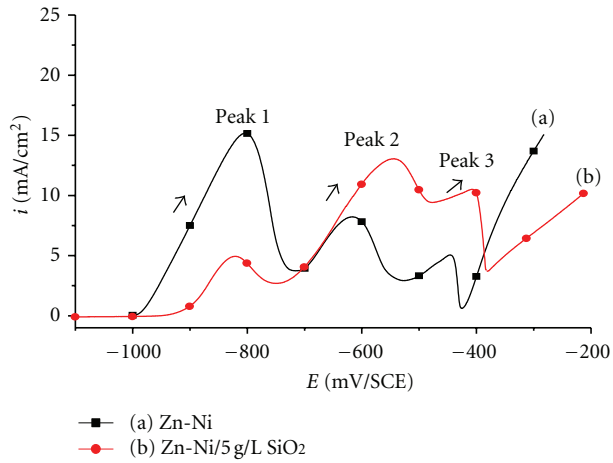

Figure 6: Anodic polarization curves of steel substrates coated with Zn-Ni alloy coating (a) and Zn-Ni alloy composite (b) elaborated under DC (25 mA/cm^2, 15 min); immersion in 3% NaCl.

3.5. Corrosion Behavior of Zn-Ni Alloy Deposits in 3% NaCl Solution

3.5.1. Potentiodynamic Polarization Studies. Figure 6 showed the anodic polarization curves elaborated at v = 25 mV/min of steel substrates coated with Zn-Ni alloy coating immerged in 3% NaCl. Distinct peaks were observed which could be attributed to the dissolution of Zn-Ni alloy components [17, 18] in the corroding media.

Based on previous results [7], we could make a qualitative estimate of Zn-Ni alloy structure. The two first peaks corresponded to the dissolution (dealloying) of Zn from η and γ phases which were situated at, respectively, −800 and −615 mV/SCE, whereas the third peak corresponded to the dissolution of Ni from their phases (Table 4). We noted that the intensity of the first peak relative to Zn-Ni alloy composite decreased. This evolution suggests a reduce of the electrochemical kinetics of Zn-Ni composite. In fact, an increase in life of the protective coating would simply depend on the life of the more electronegative phase, which is a Zn-rich η phase [19]. Dissolution of this phase would expose the nickel-rich phase to the environment.

As mentioned in Table 4, there was a clear shift for second and third peaks toward the noble direction (Table 4), giving rise to an increase in corrosion resistance of Zn-Ni composite coating. Moreover, the corrosion potential shifted to positive values (Table 4) indicating a change in the content ratio in the alloy and higher corrosion resistance compared with the Zn-Ni alloy coating.

We followed the loss of metal from Zn-Ni alloy deposit by stripping with X-ray fluorescence. In comparison with Zn-Ni alloy coatings, we noted that the dezincification rate of Zn-Ni alloy composites decreased from 24% to 2% until the last remaining phase (α-phase).

3.5.2. Electrochemical Impedance Spectroscopy. EIS was used to evaluate the barrier properties of the coatings after 24 hours of immersion in 3% NaCl and to determine their polarization resistance. Figure 7(a) presented a comparison of Nyquist responses obtained for Zn-Ni alloy coatings and Zn-Ni alloy composites elaborated under the same quantities of electricity. Three semicircles are generally observed in the complex-plane representation of the EIS data; the enlargement of the curves at high frequency (Figure 7(b)) showed the third semicircle.

The Nyquist-like diagram of the samples is characteristic of electrode process under kinetic and charge transfer control. The polarization resistance values could be approximately determined by fitting the Nyquist response to an equivalent circuit consisting of three RC components: the first

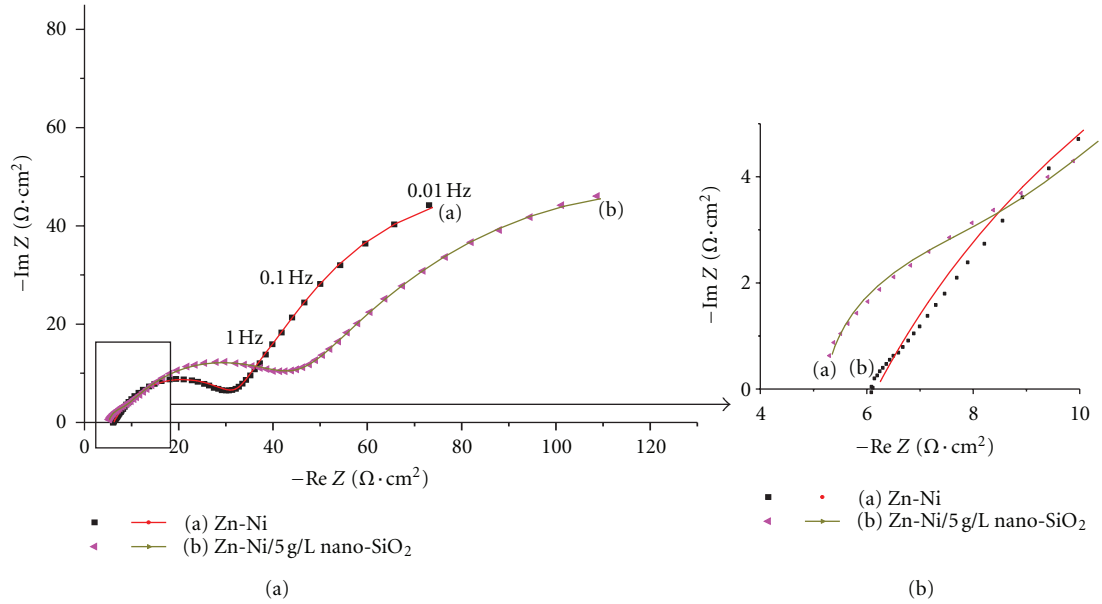

Figure 7: Nyquist plots obtained for Zn-Ni alloy coating (a) and Zn-Ni alloy composite (b), after 24 h immersion in 3% NaCl solution. Symbols are the experimental data, and lines were modeled using fitting model.

Table 5: Data obtained by electrochemical impedance spectroscopy of coatings immersed in 3% NaCl solution for 24 h.

Coating systems	R_{pc} (ohm · cm^2)	C_c (F · cm^{-2})	R_p (ohm · cm^2)	Composition analyses (±0.2 wt.%)				
				Zn	Ni	Cl	Fe	Si
Zn-Ni alloy coating	0.4	10^{-5}	320	71	6	10.8	1.30	—
Zn-Ni alloy composite	6.5	3×10^{-6}	560	85.5	9.73	4	0.47	0.8

time constant (R_{pc}, C_c) was attributed to the protective coating properties, (R_t, C_{dl}) an intermediate relaxation attributed to charge transfer which produced in the film defaults with R_t was the charge transfer resistance, and C_{dl} was the double-layer capacitance at the interface. This time constant was probably due to the heterogeneity of the film which can result from the existence of high- and low-density zones inside the film. The third time constant (R_F, C_F) in the low-frequency part (1–10^{-2} Hz) could be attributed to the deposited corrosion products [20]. In all cases, the proposed model was in total agreement with the experimental data. The R_p values of Zn-Ni alloy coatings, determined by fitting with the model and summarized in Table 5, was estimated from the addition of (R_{pc} + R_t + R_F). From Table 5, we noted that R_{pc} values of this system, which reached 6.5 Ω·cm^2, were seen to improve, while their capacitance C_c decreases. In the meantime, we noted an increase of R_p value of Zn-Ni alloy composite denoting the decrease of the corrosion intensity.

Composition analyses of deposits immersed in 3% NaCl for 24 h (Table 5) showed that composites dissolve slower than Zn-Ni alloy coatings and keep a higher percentage of Ni in the deposit.

MEB micrographs indicated that Zn-Ni alloy coating immersed in 3% NaCl for 24 hours suffered from defects with grains of salt deposited in clusters on the surface (Figure 8(a)). However, micrographs of Zn-Ni alloy composite showed a reduction in the defects sizes (Figure 8(b)) and the deposit seemed to keep the same appearance represented in Figure 1(b). EDS analysis showed that the nanoparticles of SiO_2 were still incorporated in the composite, while their percentage decreased to 0.8%. In fact, the incorporation of nanoparticles in the deposit may be helpful to segregate the corrosion products appeared in a thin layer in Figure 8(b). This is confirmed by composition analyses showed in Table 5, which proved a decrease of the percentage of Fe and Cl in the composite in comparison with Zn-Ni alloy coating. Several hypotheses have been developed assuming that the decrease of corrosion intensity may be related to the structural and/or electronic properties of the passive oxide particles [21].

4. Conclusion

This work represented the electrodeposition and the corrosion behavior of Zn-Ni alloy deposits elaborated in absence or in presence of 5 g/L of nano-SiO_2 in the plating bath. This study was made to evaluate the influence of nanoparticles addition on some properties such as hardness, morphologic,

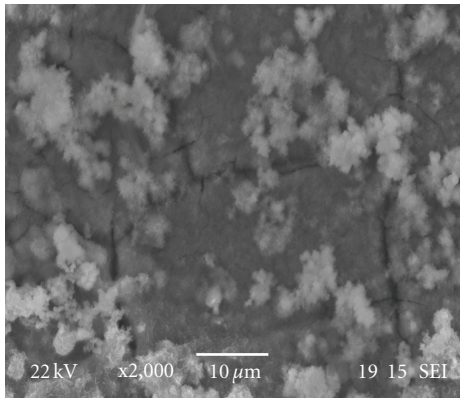

(a)

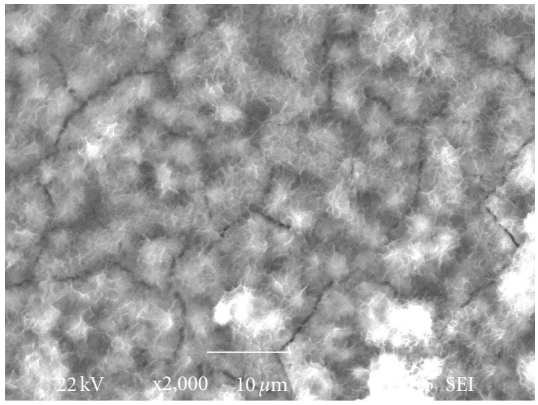

(b)

Figure 8: Comparison of SEM micrographs of the surfaces of deposits elaborated at 25 mA/cm^2 for 15 min onto steel substrate and immerged for 24 hours in 3% NaCl solution: (a) Zn-Ni alloy coating, (b) Zn-Ni alloy composite.

structure characteristics, and corrosion resistance. In comparison with Zn-Ni alloy coatings, the results revealed that Zn-Ni alloy composites:

(i) revealed a higher percentage of Ni and an incorporation of 1.54% of silica in the deposit,

(ii) formed a mixture of two phases, zinc and γ phases, with smaller crystallite size,

(iii) exhibited higher values of microhardness and were thermally stable up to 24 hours at 200°C,

(iv) revealed better corrosion resistance in corrosive media of 3% NaCl. This behavior indicates that Ni content, morphology, and the content of nanoparticles in the composite are responsible for the observed corrosion behavior.

Acknowledgments

The authors would like to acknowledge the financial support provided by "Action Intégrée Franco-Tunisienne du Ministère des Affaires Etrangères et Européennes Français et du Ministère de l'Enseignement Supérieur, de la Recherche Scientifique et de la Technologie Tunisien."

References

[1] E. A. Pavlatou, M. Stroumbouli, P. Gyftou, and N. Spyrellis, "Hardening effect induced by incorporation of SiC particles in nickel electrodeposits," *Journal of Applied Electrochemistry*, vol. 36, no. 4, pp. 385–394, 2006.

[2] P. Gyftou, M. Stroumbouli, E. A. Pavlatou, P. Asimidis, and N. Spyrellis, "Tribological study of Ni matrix composite coatings containing nano and micro SiC particles," *Electrochimica Acta*, vol. 50, no. 23, pp. 4544–4550, 2005.

[3] N. K. Shrestha, D. B. Hamal, and T. Saji, "Composite plating of Ni–P–Al_2O_3," *Surface and Coatings Technology*, vol. 183, no. 2-3, pp. 247–253, 2004.

[4] S. Kim, J. J. Gislason, R. W. Morton, X. Q. Pan, H. P. Sun, and R. M. Laine, "Liquid-feed flame spray pyrolysis of nanopowders in the alumina-titania system," *Chemistry of Materials*, vol. 16, no. 12, pp. 2336–2343, 2004.

[5] P. A. Janeway, "Nanotechnology—it's more than size," *American Ceramic Society Bulletin*, vol. 82, no. 4, pp. 31–38, 2003.

[6] B. Losiewicz, A. Stępień, D. Gierlotka, and A. Budniok, "Composite layers in Ni-P system containing TiO_2 and PTFE," *Thin Solid Films*, vol. 349, no. 1, pp. 43–50, 1999.

[7] O. Hammami, L. Dhouibi, and E. Triki, "Influence of Zn-Ni alloy electrodeposition techniques on the coating corrosion behaviour in chloride solution," *Surface and Coatings Technology*, vol. 203, no. 19, pp. 2863–2870, 2009.

[8] A. Hovestad and L. J. J. Janssen, "Electrochemical codeposition of inert particles in a metallic matrix," *Journal of Applied Electrochemistry*, vol. 25, no. 6, pp. 519–527, 1995.

[9] M. Azizi, W. Schneider, and W. Plieth, "Electrolytic co-deposition of silicate and mica particles with zinc," *Journal of Solid State Electrochemistry*, vol. 9, no. 6, pp. 429–437, 2005.

[10] P. C. Hiemenz, *Principles of Colloid and Surface Chemistry*, vol. 2, Marcel Dekker, 1986.

[11] A. M. Alfantazi, A. M. El-Sherik, and U. Erb, "The role of nickel in the morphology evolution of pulse plated ZnNi alloy coatings," *Scripta Metallurgica et Materiala*, vol. 30, no. 10, pp. 1245–1250, 1994.

[12] T. R. Khan, A. Erbe, M. Auinger, F. Marlow, and M. Rohwerder, "Electrodeposition of zinc-silica composite coatings: challenges in incorporating functionalized silica particles into a zinc matrix," *Science and Technology of Advanced Materials*, vol. 12, no. 5, Article ID 055005, 2011.

[13] A. Brenner, *Electrodeposition of alloys, Principles and Practice*, vol. 2, Academic Press, 1963.

[14] H. P. Klug and L. E. Alexander, *X-Ray Diffraction Procedures*, vol. 7, Chapman and Hall, 1959.

[15] A. Portinha, V. Teixeira, J. O. Carneiro, S. N. Dub, R. Shmegera, and C. J. Tavares, "Hard ZrO_2/Al_2O_3 nanolaminated PVD coatings evaluated by nanoindentation," *Surface and Coatings Technology*, vol. 200, no. 1–4, pp. 765–768, 2005.

[16] I. Apachitei, F. D. Tichelaar, J. Duszczyk, and L. Katgerman, "The effect of heat treatment on the structure and abrasive wear resistance of autocatalytic NiP and NiP-SiC coatings," *Surface and Coatings Technology*, vol. 149, no. 2-3, pp. 263–278, 2002.

[17] S. K. Zečević, J. B. Zotović, S. Lj. Gojković, and V. Radmilović, "Electrochemically deposited thin films of amorphous Fe-P alloy Part I. Chemical composition and phase structure characterization," *Journal of Electroanalytical Chemistry*, vol. 448, no. 2, pp. 245–252, 1998.

[18] S. Swathirajan, "Electrodeposition of zinc + nickel alloy phases and electrochemical stripping studies of the anomalous

codeposition of zinc," *Journal of Electroanalytical Chemistry*, vol. 221, no. 1-2, pp. 211–228, 1987.

[19] M. M. Abou-Krisha, H. M. Rageh, and E. A. Matter, "Electrochemical studies on the electrodeposited Zn-Ni-Co ternary alloy in different media," *Surface and Coatings Technology*, vol. 202, no. 15, pp. 3739–3746, 2008.

[20] D. Zhu and W. J. van Ooij, "Corrosion protection of AA 2024-T3 by bis-[3-(triethoxysilyl) propyl]tetrasulfide in sodium chloride solution.Part 2: mechanism for corrosion protection," *Corrosion Science*, vol. 45, no. 10, pp. 2177–2197, 2003.

[21] M. A. M. H. Al-Rabea, F. F. M. Saeed, A. W. K. Rajih, and F. M. Hussoun, "Using (Zn-Ni-SiO_2) electrocomposite coating to prevent carbon steel against acidic environments," Conference Paper, Corrosion in Babylon University Atlanta, 6 pages, March 2009.